Electronic Supplementary Material (ESI) for Nanoscale.
This journal is © The Royal Society of Chemistry 2017

Granular topological insulators: Supplementary Information

I. GROWTH AND CHARACTERIZATION OF THIN FILMS

Thin films of Bi_2Se_3 nanocrystals are grown on high resistivity Si(111) substrates using pulsed laser deposition. A KrF excimer laser source (Coherent, GmBh) is used while the chamber pressure is kept constant at 10^{-5} mbar. Deposition at high laser energies gives rise to thin films oriented along the c-axis but with a large degree of granularity. To quantify this, we perform azimuthal X-ray scans on the asymmetric (105) family of planes belonging to Bi_2Se_3 as shown in the inset of Fig. 3 (b) in the main paper. While the six-fold symmetry is still preserved, the large degree of peak broadening (FWHM $\sim 8^\circ$) represents in-plane misorientations between neighboring Bi_2Se_3 monolayers (quintuples). This is further confirmed by symmetric reciprocal space map on the (003) peak of Bi_2Se_3 respectively (Fig. 3 (c)). The broadening of the reciprocal lattice peak can be used to obtain the coherence lengths of granules in the in-plane and out-of-plane directions. The inverse FWHMs of Q_x and Q_z give the in-plane and out-of-plane coherence lengths respectively. Our measurements indicate an in-plane coherence length $\xi_\parallel \approx 10$ nm, which is somewhat smaller than the grain width estimated from AFM $\sim$ 20-25nm. The out-of plane coherence length is estimated as $\xi_\perp \approx 2-3$ nm, which is a result of larger Q_z broadening. From a growth point of view, this is a consequence of the Van der Waals bonded nature of the material. The film grows much faster in the lateral directions, owing to the larger number of lateral dangling bonds, than in the vertical c-axis direction where the bonding is of the Van der Waals type.

To quantify the out-of-plane grain size further, we performed AFM measurements on thin films that are not granular, and instead exhibit a spiral surface morphology with large terrace widths (Fig. S1). Such a growth morphology is typical for thin films reported elsewhere [1, 2]. In these films, we typically observe a vertical height of ~ 5 nm visible as individual quintuple layers, for an in-plane grain size of ~ 100 nm. This means that the growth rate for these samples is around 20 times larger in the in-plane direction than in the vertical direction. For granular films we have a thin film growth rate of 60 pulse/nm, while the more crystalline films as shown in Fig. S1 are grown at 250 pulse/nm. A simple calculation yields that for a horizontal grain size of roughly 10 nm, the vertical grain size for a granular sample should be ~ 2 nm. Our thin films are therefore composed of highly ordered aggregates of nanocrystals, where each nanocrystal grain behaves like a quantum dot (Fig. 3 (a)). To verify whether sample thickness affects the granular morphology of our samples, we performed reciprocal

space map measurements of the (003) peak of Bi_2Se_3 on granular TI samples with different thicknesses(Fig. S2(a)(b)). We do not observe any change in the peak broadening over an order of magnitude change in thickness confirming that the grain size does not change with increasing sample thickness. AFM images of the surface topography of samples with different thicknesses also show no significant change(Fig. S2(c)-(e)).

The thickness of our films is changed by altering the number of laser pulses. Although the granular packing is uniform, we expect an asymmetry in the inter-grain couplings. While the in-plane coupling is expected to be strong due to a large density of lateral dangling bonds, the absence of dangling bonds in the vertical directions makes the vertical inter-grain coupling weak.

II. TWO-DIMENSIONAL WEAK ANTILOCALIZATION FITTING

The perpendicular field magnetoconductance (MC) data are fitted to the Hikami-Larkin-Nagaoka (HLN) equation that quantifies the conductance correction due to weak antilocalization (WAL) in two dimensions,

$$\Delta\sigma_\perp(B_\perp) = -\alpha_\perp \frac{e^2}{2\pi^2\hbar}\left[\psi\left(\frac{1}{2}+\frac{\hbar}{4el_\phi^2 B_\perp}\right) - \ln\left(\frac{\hbar}{4el_\phi^2 B_\perp}\right)\right] \tag{1}$$

in the limit of strong spin-orbit scattering, where σ is the sample conductivity, $B_\perp$ is the applied magnetic field, e is the electronic charge, $\hbar$ is Planck's constant, l_ϕ is the phase coherence length, and $\psi(x)$ represents the digamma function. For performing the fit, the data is presented in the form of $\Delta G(B_\perp) = G(B_\perp) - G(0)$, where G is the two-dimensional (2D) sample conductivity obtained from the sample conductance by taking the sample aspect ratio W/L into account. For all our samples, L/W is close to 2.0. While performing the fit, the classical contribution to the magnetoresistance ($\propto B_\perp^2$) due to orbital motion is also taken into account. This model gives reasonably good fits for the thick film samples ($t > 60$ nm) (Fig. S3 (a)). More specifically, the 2D WAL model fits our data up to fields as high as 8 T with almost negligible orbital magnetoresistance (MR) contributions. The extracted phase coherence length l_ϕ is shown in Fig. S3 (b).

The case of in-plane magnetic fields is more complicated. Previous parallel field MR measurements on topological insulators (TIs) have yielded ambiguous results. In these experiments, it is not clear whether the MR contributions arise from the surface states

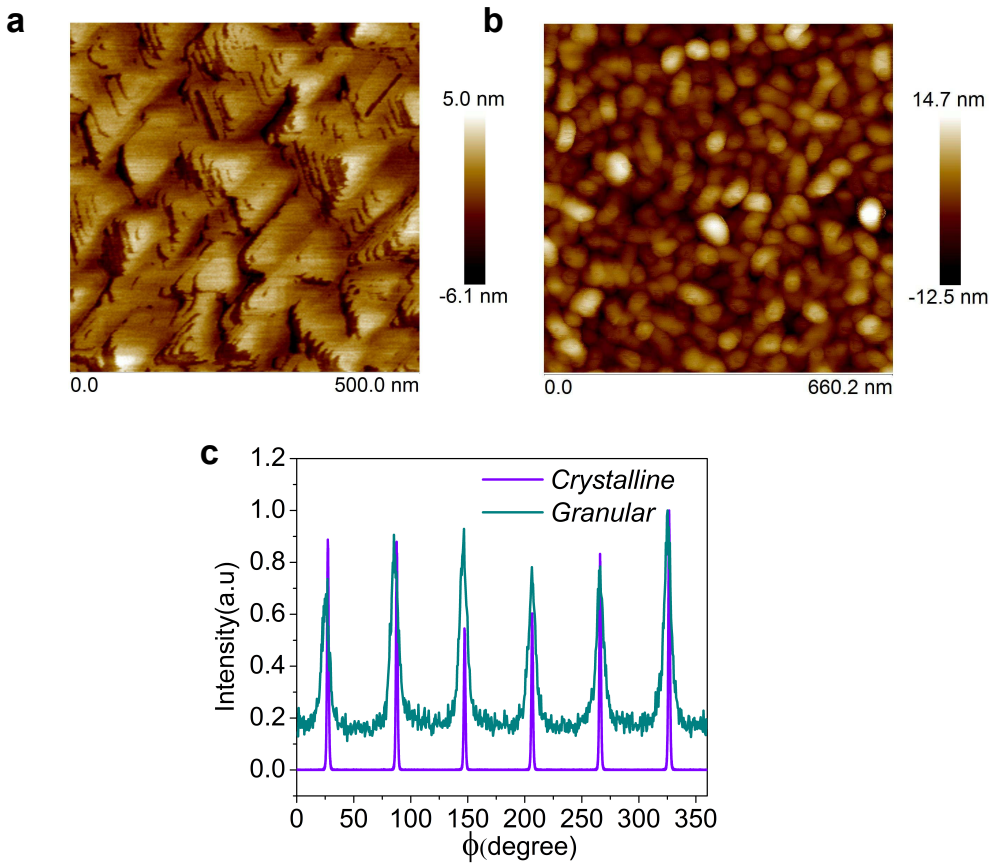

FIG. S1: **Growth of granular TI thin films.** (a) Topography image of a highly crystalline thin film measured with an AFM. The step-terrace morphology exhibits a spiral structure with a monolayer (quintuple) height of $\sim$ 1 nm. (b) Topography of granular TI film with a significantly smaller lateral grain size. (c) X-ray diffraction azimuthal scan of {105} planes for granular and crystalline thin films. The granular films exhibit significantly larger broadening implying large in-plane misorientation.

penetrating into the bulk, or the bulk states, or a combination of the two. For the case of ideal TIs with perfectly 2D surface states, in-plane fields cannot interact with the surface states and therefore provide no contribution to the MR. However, the finite penetration of the surface states into the bulk allows an interaction with in-plane fields that can effectively be used to estimate the surface state penetration depth. Our measurements reveal an unusually large parallel field MR, with magnitudes comparable with the perpendicular field MR. The MR obtained in the parallel field configuration is fitted using the WAL formula modified for

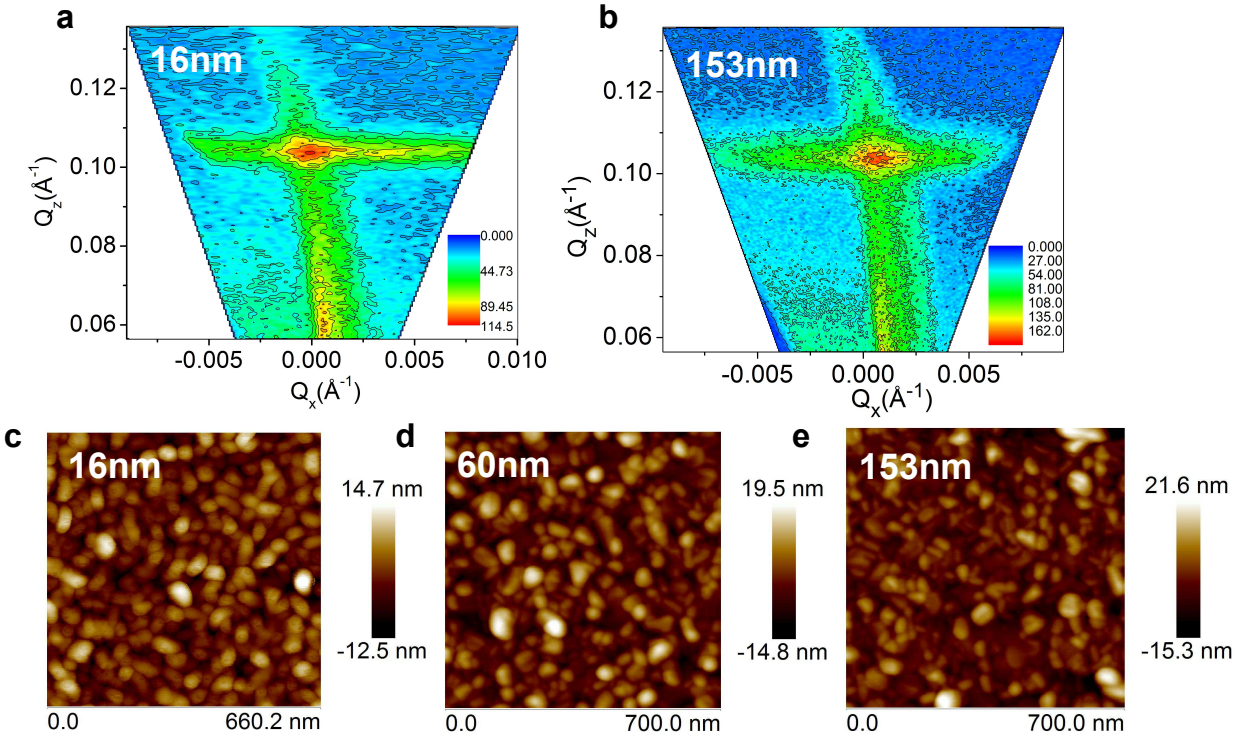

FIG. S2: **Thickness independence of thin film growth morphology** Reciprocal space map of the (003) peak of Bi_2Se_3 for samples with thickness (a) 16nm and (b)153nm. AFM image showing the surface topography of samples with thickness (c) 16nm, (d) 60nm and (e) 153nm.

the case of in-plane fields:

$$\Delta\sigma_{\parallel}(B_{\parallel}) = -\alpha_{\parallel}\frac{e^2}{2\pi^2\hbar}\ln\left(1+B_{\parallel}^2/B_{\phi}^2\right), \tag{2}$$

where $B_\phi = \hbar/(e\lambda l_\phi)$ and λ is the surface state penetration depth. In fitting our data, we take $\alpha_{\parallel}$ and λ as the fitting parameters while the phase coherence length l_ϕ is used as extracted from the perpendicular field data. We assume that the phase coherence lengths for the perpendicular and parallel field measurements must be the same if the contributions to the conductance corrections come from the same channels in both cases. We find that the values obtained for $\alpha_{\parallel}$ match closely the values obtained for $\alpha_{\perp}$ for all ranges of temperature and sample thickness. Further, the thickness dependent cross-over from 0.5 to 1 is observed for both $\alpha_{\perp}$ and $\alpha_{\parallel}$, indicating the consistency of our fits and justifying the usage of the same l_ϕ for both the fittings. The large values of λ indicate a large penetration depth of surface states and explains why the in-plane MR is anomalously high.

We can explain the non-monotonic dependence of the in-plane MR on thickness as follows.

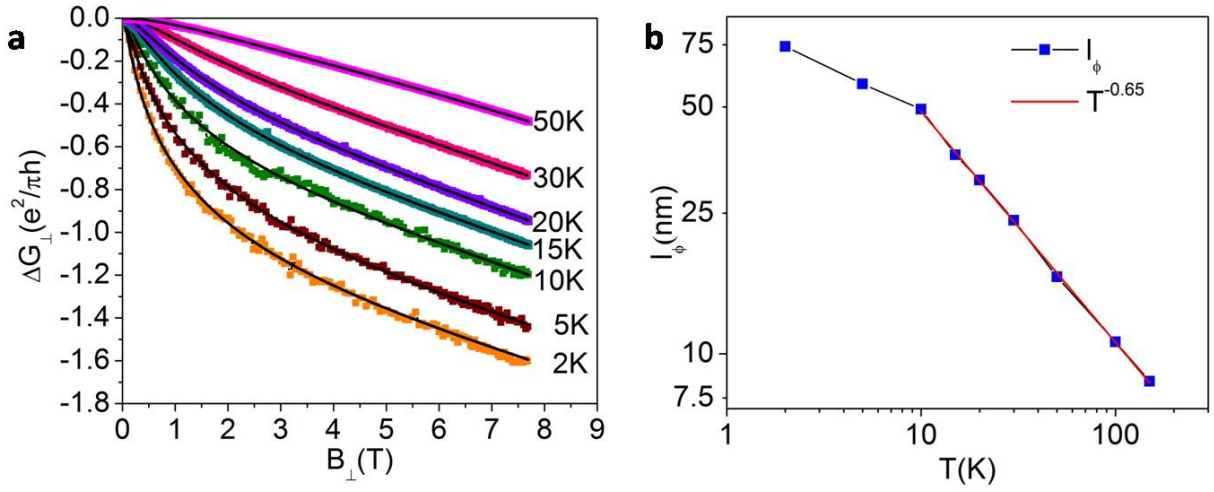

FIG. S3: **Two-dimensional Weak Antilocalization.** (a) 2D WAL fitting of the perpendicular field MC for $t = 153$ nm. (b) Phase coherence length as a function of temperature as extracted from the WAL fitting.

The in-plane MR is a combination of two factors. First, it depends on λ; larger values of λ result in a larger in-plane MR. Secondly, it scales with $\alpha_{\|}$. Therefore a competition between λ and $\alpha_{\|}$ determines the magnitude of the in-plane MR and gives rise to a non-monotonic dependence on the thickness.

In Fig. S4 we show the MC data and the corresponding fittings in both in-plane and out-of-plane field configurations for different sample thicknesses and temperatures. All samples indicate qualitatively similar behaviors showing a sharp negative MC, with the signal becoming weaker with increasing temperature. The experimental data is symmetrized and then fit to the appropriate MC formulae. Our models fit our experimental data very accurately for a variety of sample thicknesses and sample temperatures. Most notably, our fitting accurately captures the physics not only in the low magnetic field regimes, in which the HLN equation in conventionally thought to work, but also in the high field regime up to 7 T.

---

[1] Y. Liu, M. Weinert, and L. Li, Phys. Rev. Lett. **108**, 115501 (2012).

[2] A. Kandala, A. Richardella, D. Zhang, T. Flanagan, and N. Samarth, Nano Letters **13**, 2471

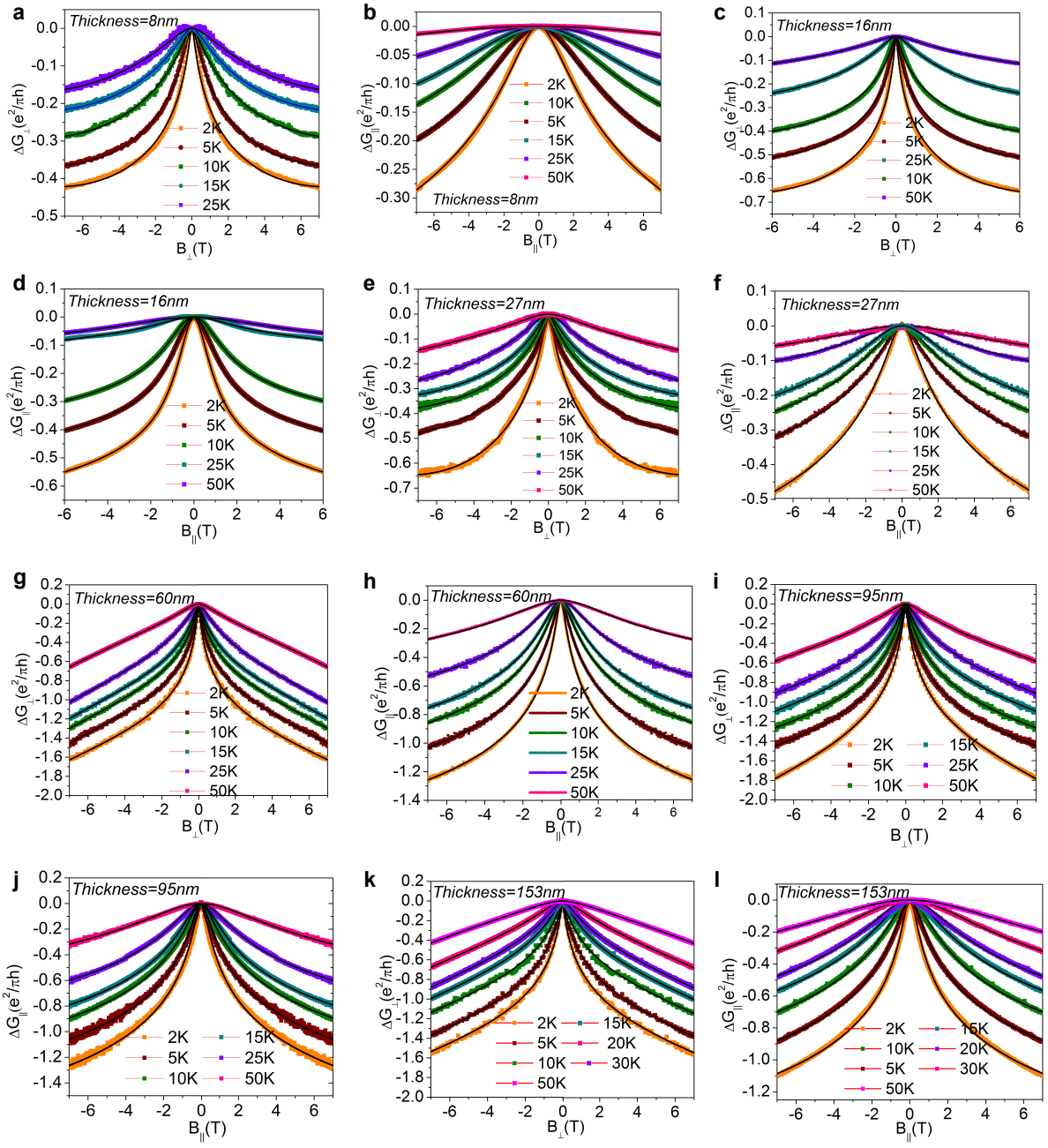

FIG. S4: **Temperature dependent MC data and fitting.** (a)-(l) Symmetrized MC as a function of temperature for different sample thicknesses. The black continuous lines superimposed on the data indicate the best fits.

(2013).